https://doi.org/10.48048/tis.2022.5533

Design and Life Cycle Cost Analysis of a Forward Converter Feded Solar Powered 3-phase Water Motor

Mohammad Shahadat Hossain[1,*], Imtiaz Akber Chowdhury[1], Rocky Chakma[1] and Ashraful Hoque[2]

[1]*Department of Electrical and Electronic Engineering, University of Science and Technology Chittagong, Chattogram, Bangladesh*
[2]*Department of Electrical and Electronic Engineering, Islamic University of Technology, Dhaka, Bangladesh*

([*]Corresponding author's e-mail: shahadat@ustc.ac.bd)

Received: 11 December 2020, Revised: 10 June 2021, Accepted: 17 June 2021

Abstract

Supply of water for irrigation and household use is not adequate in rural Bangladesh during dry season. To ensure continuous water supply for irrigation and other household activities in rural Bangladesh, where the supply of uninterrupted electricity is hardly available all the time and mostly irrigation is done by Diesel-based water pump. The paper proposes a standalone model to run a 3-phase motor in such condition. Due to the continuous reduction of price of electrical and electronic components related to solar panel, solar based pumping system has become the most economically viable option to mitigate this problem related to larger rural community. Output from the solar cell is converted to stable high DC voltage by incorporating a single stage forward converter. Switching circuit for 3-phase inverters is simulated in Power Sim (PSIM) which maintains the smooth operation of the water motor. The T-LCL filter is introduced to reduce the voltage ripple to a tolerance level before being fed to the motor. Forward converter based proposed system has a better total harmonic distortion (THD) of 0.087 with different output voltage as required. The conventional Diesel-based system not only pollutes the environment but also the total of capital investment and maintenance cost is more than 3 times higher than the proposed Forward converter and 3-phase sinusoidal pulse-width modulation (SPWM) inverter-based system. This model can be a good solution considering the unavailability, high price and environmental issues of fuel-based power supply.

Keywords: Filters, Forward converter, Lifecycle cost analysis, Pulse-width modulation, Standalone model, Third harmonic distortion (THD), 3-phase motor

Introduction

Electrical energy has been the prime factor for the development since the day of industrial revolution. The demand for electrical energy has also been increasing ever since. The rate of increase in this demand is twice as compared to other energy in the same period. Another point which needs to be taken care off is the ever increasing demand of the overpopulated countries like Bangladesh. There is also huge inefficiency in supplying power to rural areas. This is where this work contributes to reduce the inefficiency of rural area by introducing advanced power electronics in the generation end [1].

Dependency on fossil fuel to fulfill the power demand is not a permanent and environment friendly solution, as power plants based on fossil fuel pollutes the environment and at the same time these resources are along decreasing at a fast pace. Moreover, countries like Bangladesh can not satisfy the increasing power demand, which causes significant problem in rural areas to perform household and agricultural activities. Average sunlight hours, cloud coverage and solar radiation in different areas of Bangladesh are suitable to implement solar energy based technology comparing with other developed countries like Germany and Spain in this regard [2].

There are many models of photovoltaic based on its operation and behavior. In general photovoltaic water pumping system (PVPS) have a number of challenges including modeling, control strategy [3]. In 1 work by Swamy *et al.* [4] described the study carried on PMBLDC (permanent magnet brushless) motors to run a water pump using solar power as the source of energy. A novel hybrid system to run a 3-phase induction motor proposed in [5]. In this hybrid system PV and battery are used to drive this motor. This incorporates a DC boost converter to use the DG as a part of unified structure. In this every switching cycle that is proposed interleaved boost converter is divided into 5 switching period that incorporates 5 different duty cycles. In another study BLDC is driven by a hybrid system [6]. The hybrid system in this work is consists off PV array, fuel cell stacks and battery. For utilizing DG sources in a unified manner, a multi-input DC boost converter has been used in HDGS system. Each switching cycle of the boost converter is again divided into 5 switching time which incorporates different 5 duty ratios. By using these DR (Duty ratio) a regulated PV/FC/Battery power is achieved. By doing this a fixed DC power is supplied to the motor.

Boost converters are used to higher the voltage level as DC-DC converter [7]. For extraction of groundwater, a dynamic model of a system considered in [8] utilize an alternative source of energy. Another similar work has been done by Kumar and B. Singh, they proposed a DC-DC boost converter as an intermediate power conditioning unit a PV array to run BLDC water pump [9]. Another system with SPWM inverter, LC filter, induction motor and a centrifugal pump is presented [10]. M.A. Rahman proposed a system in which induction motor integrates a push pull converter and a 3-phase inverter, the system is driven by a single solar PV [11].

An efficient and cost-effective configuration is needed [12-15] where several configurations are possible for DC-DC conversion like DC-to-DC forward, DC to DC boost, DC to DC fly-back and DC to DC push-pull converter [16-19]. The proposed system suggests a forward converter in order to raise the DC voltage from 48 V-DC to 312 V-DC, as the other alternate configurations like push-pull, flyback or boost converter has limitation considering the current harmonics of high frequency. Many researchers introduced PWM inverter in the system [20-22] for the control of induction motor. But it does have many drawbacks like low fundamental output voltage, large amount of harmonics and higher total harmonic distortion are the main issues with this technique. To Combat this issue, SPWM (Sinusoidal Pulse Width Modulation) has been taken into account [23]. Total cost during life cycle of this system has been analyzed to assess the economic feasibility[24]. Then the proposed system is compared with a traditional carbon-fuel based system [25].

Material and methods

The mathematical model of the system is studied and simulated via PSIM. Result has been tallied to validate the proposed system. The primary objective of this work is to produce a DC-AC inverter where AC output will be greater than the DC input and can provide a much sound technical and economic model over the existing VSL.

System design flowchart

1) From **Figure 1**, a DC-DC forward converter have been designed to convert unregulated PV output to a regulated voltage. Voltage level that has been determined is 312V peak or 220V RMS. The source voltage of 48V DC has been stepped up to 312V DC by the forward converter.

2) A 3-phase inverter have been proposed with SPWM switching states which are suitable for the smooth operation of a 3-phase motor, and to ensure a continuous supply of power to the motor.

3) A T-LCL filter circuit have been implemented to ensure the elimination of the harmonics from the inverter output and the results have been compared in PSIM.

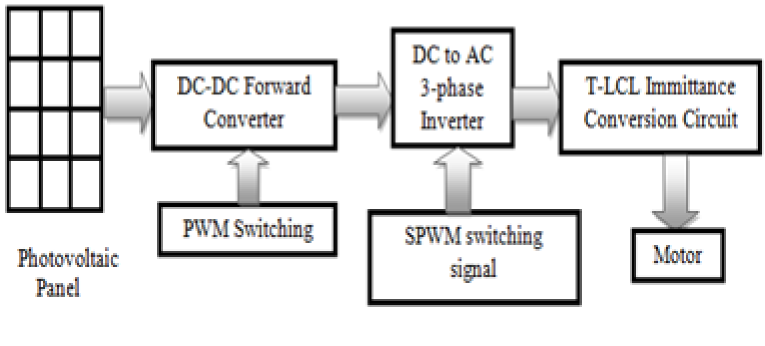

Figure 1 Block diagram of the proposed PV system.

Design of a solar panel

At Standard Test Condition (STC), a solar panel of 250W power is assessed at 250, when the irradiance is 1,000 W/m^2, specifications of a PV module is shown in **Table 1**.

Table 1 Photovoltaic module specifications.

Specification	Value
Fabricator	Sanyo
PV model	HIP-210HKHA6
Maximum power (Pmax) of solar panel	250 W
Current (I) at short circuit	8.96 A
Voltage (V) at open circuit	37.33 V
Characteristic constant (b)	0.0773
Solar panel efficiency	17.95 %
Type of cell	156×156

Design of forward converter

A forward converter consists of a transformer (ferrite core) and a PWM gate pulses to operate the MOSFET. This type of converter can supply voltage higher than the input and it provides electrical isolation [26,27]. It is also a good option when high output current is required.

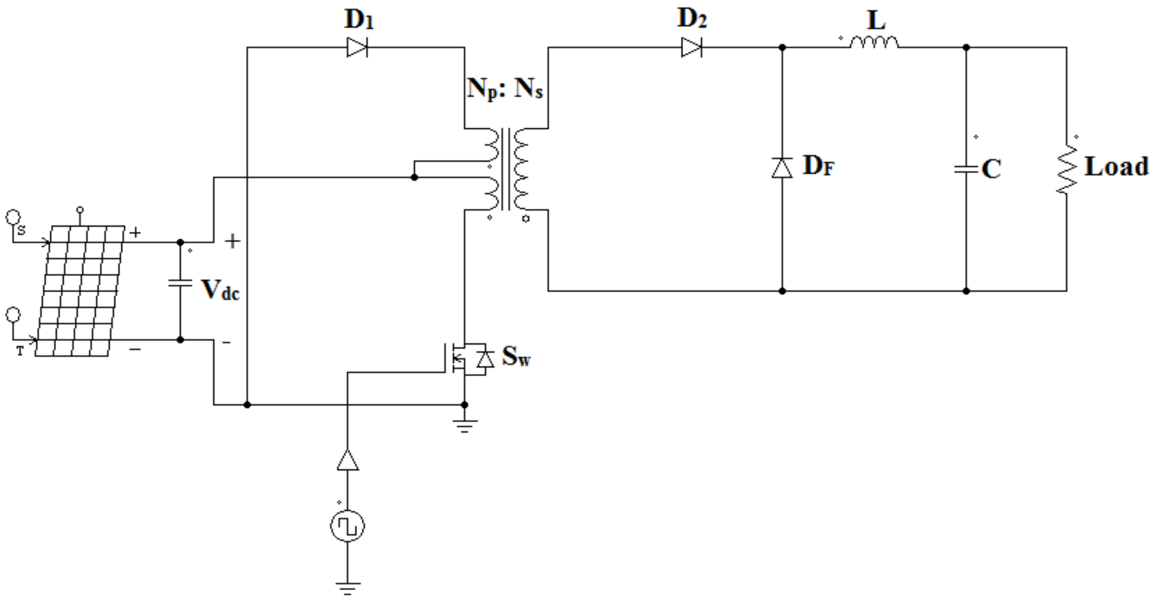

Figure 2 Forward converter circuit at PSIM simulation software.

Table 2 Forward converter specifications.

Specification	Value
Duty cycle (D)	0.36 s
Filter capacitance (C) at output	1 mf
Inductor (L) at secondary	1.85 mH
Simulation time (T)	0.2 s
Switching frequency (fs)	20 KHz
Turn ratio (n)	21

Transformer primary winding has been connected in series with the MOSFET Sw, and the secondary winding has been connected to an output LC filter. To prevent the negative current flow in the secondary winding of the transformer, diode D_2 is used, while diode D_F is exploited as a free-wheeling diode. When the MOSFET Sw is conducting, the voltage V_1 = Vdc, while MOSFET Sw is not conducting, the voltage is given by $V_1 = V_2 = 0$.

SPWM inverter

As the inverters employ switching devices with a fixed ON-OFF time, hence the loss in this is quite natural as a result of which efficiency, size and reliability is strongly affected. For this system SPWM has been considered because of its wide variety of advantages [28].

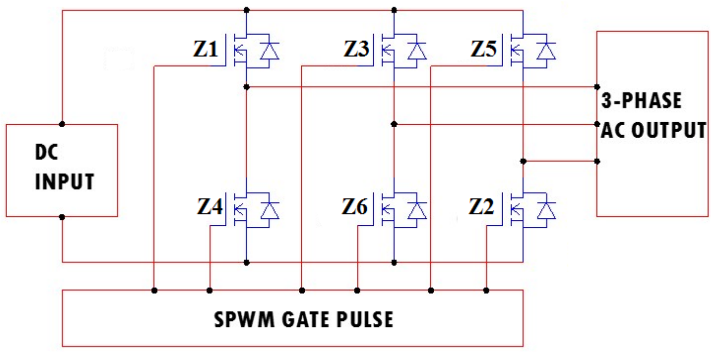

Figure 3 SPWM inverter circuit.

SPWM is used to keep the output voltage stable even though the load varies. In order to combat this SPWM inverters compensate the O/P voltage in accordance to the load connected by changing the pulse width of the switching frequency which is generated by the oscillator. This is done by a feedback loop which is connected to the inverter controller. After the controller gets the O/P voltage through the feedback path, it corrects the pulse width so that the output voltage is always stable. This phenomenon is called pulse width modulation (PWM). If a reference signal is used in the generation of pulse, then it is called SPWM. [29]

Switching circuit design

Three sinusoidal reference waves which are phase shifted from each other by an angle of 1,200 are considered for 3-phase inverters. A carrier wave, vcarrier of 20 KHz is then compared with Vr, Vg, Vb analogous to a phase to initiate the gate signals for the respective phase. Comparing carrier wave with sinusoidal reference waves generates Z1, Z3 and Z5 switching signals separately. Z2, Z4 and Z6 are the corresponding inverted gate switching signals. **Figure 4** presents the design of 3-phase circuitry.

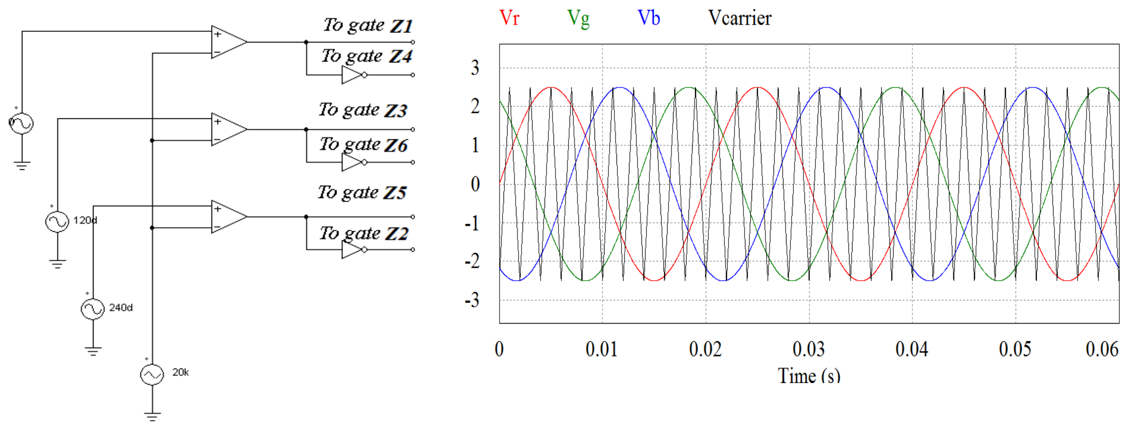

Figure 4 Control circuit of proposed 3-phase inverter and SPWM gate driver signal.

Table 3 shows 6 modes of operations, achieved from different combinations of switches. Switching State has logic of ‘1’ if the MOSFET that connects the motor to the positive terminal is switched ‘ON’, and vice versa. From left to right, switching state 3 bits corresponds to the state of the MOSFETS in the following order: Z1, Z3, and Z5.

Table 3 List of inverter switching states.

List of states	State	Switching state	Vab	Vbc	Vca
1	Z1, Z4, Z6 on Z2, Z3, Z5 off	100	Vdc	0	−Vdc
2	Z1, Z3, Z6 on Z2, Z4, Z5 off	110	0	Vdc	−Vdc
3	Z2, Z3, Z6 on Z1, Z4, Z5 off	010	−Vdc	Vdc	0
4	Z2, Z3, Z5 on Z1, Z4, Z6 off	011	−Vdc	0	Vdc
5	Z2, Z4, Z5 on Z1, Z3, Z6 off	001	0	−Vdc	Vdc
6	Z1, Z4, Z5 on Z2, Z3, Z6 off	101	Vdc	−Vdc	0
7	Z1, Z3, Z5 on Z2, Z4, Z6 off	111	0	0	0
8	Z2, Z4, Z6 on Z1, Z3, Z5 off	000	0	0	0

Another point to note is that the switch state transitions in “grey code” format. In this format, the Hamming distance between any 2 successive states is 1, which means that any 2 successive states differ only by 1 bit. Thus, the states switch in the following order:

- 100 -> 110 -> 010 -> 011 -> 001 -> 101 -> 100 -> and so on for the motor rotating in 1 direction, and
- 100 -> 101 -> 001 -> 011 -> 010 -> 110 -> 100 -> and so on for the motor rotating in the opposite direction.

This switching process of is necessary for the smooth operation of the 3-phase motor, and to ensure the steady power supply to the motor. State 7 is utilized for dynamic braking of the motor, while State 8 is a free-wheeling mode, where the power supply to the motor is turned off, and the motor will slowly come to stop. During switching, voltage a terminal A, B, and C of the motor is determined by state of MOSFETs Z1, Z3, and Z5. For example, if Z1 is turned on, then terminal A will have V_{DC}, else it will have GND (or 0V). A final point to note is the potential difference between the terminals is given as A in relation to B (Vab), B in relation to C (Vbc), and C in relation to A (Vca).

T-LCL filter design

A T-LCL immitance filter which consists of 2 inductors L_1 and L_2 and a capacitor C in a T shape is employed [30] to eliminate harmonics rather than employing the conventional LC filter; as with the rise of power stresses in LC filter, the value of L increases which makes the system expensive also [31]. In the inverter side, the inductor attached is L_1. Inductor L_2 and a capacitor C_f which are in series with the damping resistor R_f, connected in the load side. Both the inductors have resistances R_1 and R_2 respectively. Inverter voltage is denoted as V_i. Again, V_g is the output system voltage. The following equation presents the transfer function:

$$H_{LCL} = \frac{i_g}{V_i} \tag{1}$$

Considering current controlled inverters and $V_g = 0$ and neglecting damping, the transfer functions become:

$$H_{LCL}(s) = \frac{1}{L_1 C_f L_2 s^3 + (L_1 + L_2)s} \tag{2}$$

If the damping resistance is considered, then the transfer function can be presented as as follows [32]:

$$Hd_{LCL}(s) = \frac{C_f R_f s + 1}{L_1 C_f L_2 s^3 + C_f (L_1 + L_2) R_f s^2 + (L_1 + L_2)s} \tag{3}$$

Base impedance and base capacitance are expressed as follows:

$$Z_b = \frac{E_n^{\ 2}}{P_n} = 176.4\,\Omega \tag{4}$$

$$C_b = \frac{1}{W_g Z_b} = 18.042\mu\text{F} \tag{5}$$

Maximum power factor variation is considered as 5 % of the grid, the base capacitance can be represented as $C_f = 0.05C_b$. Maximum current ripple from the output of inverter is described as follows:

$$\Delta I_{L\max} = \frac{2\text{V}_{DC}}{3\text{L}_1}(1-m)mT_{sw} = 0.214\text{A} \tag{6}$$

If the rated current has 10% ripple, then $\Delta I_{L\max} = 0.1 I_{\max}$

$$I_{\max} = \frac{P_n \sqrt{2}}{3\text{V}_{ph}} = 2.143\text{A} \tag{7}$$

Rated active power is presented as P_N. V_{PH} is inverter output phase voltage.

LCL filter ensures the current ripple value of 2 %. Relation between the harmonic current of the inverter and is expressed by the following equation [24]:

$$\frac{i_g(h)}{i_i(h)} = \frac{1}{|1 + r(1 - L_1 C_b w_{sw}^2 x|} = k_a = 0.02 \tag{8}$$

Inverter side inductor is termed as L_1, and can be expressed as follows:

$$L_1 = \frac{V_{DC}}{6f_{sw} \ I_{Lmax}} = 1.867\text{mH} \tag{9}$$

Here, the switching frequency is f_{sw} and V_{DC} is DC link voltage:

$$T_{sw} = \frac{1}{f_{sw}} \tag{10}$$

$$T_g = \frac{1}{f_g} \tag{11}$$

Following parameters are considered to design the Filter, which are shown in **Table 4**.

Table 4 T-LCL Filter parameters.

Symbol	Parameter definition	Value
L_1	Inverter Side Inductor	1.867 mH
L_2	Load Side Inductor	3.580 mH
C_f	Load Side Capacitor	0.902 uF
f_G	Frequency of Grid	50 Hz
f_{SW}	Switching Frequency	20 kHz
V_{LL} or E_N	RMS voltage (Line to Line)	420 V
V_{PH}	Inverter Output RMS Phase voltage	220 V
P_N	Rated active power	1,000 W
V_{DC}	DC link voltage	48 V

$$w_g = 2\pi f_g = 314.15 \ \text{radians} \tag{12}$$

$$w_{sw} = 2\pi f_{sw} = 126{,}660 \ \text{radians} \tag{13}$$

Grid side inductor is L_2 and expressed as follows: (here the desired attenuation is k_a)

$$L_2 = \frac{\sqrt{\frac{1}{k_a^2}} + 1}{C_f w_{sw}^2} = 3.580\text{mH} \tag{14}$$

The ratio of inductor L_1 and L_2 is expressed by the constant term R and expressed as follows:

$$R = \frac{L_2}{L_1} = 1.917\Omega \quad (15)$$

To avoid the resonance, a damping resistor (R_f) is introduced which is series connected with the C_f.

$$w_{res} = \sqrt{\frac{L_1 + L_2}{L_1 L_2 C_f}} \approx 31000 \text{ radians} \quad (16)$$

$$f_{res} = \frac{w_{res}}{2\pi} \approx 5000 Hz \quad (17)$$

$$R_f = \frac{1}{3 w_{res} C_f} = 12.318\,\Omega \quad (18)$$

$$C_f = \frac{1}{3 w_{res} R_f} = 0.902 \mu F \quad (19)$$

Three phase induction motor design

An induction motor is a synchronous AC machine, which has a stator and a rotor. A sinusoidal voltage is applied to the stator of induction motor, which results in an induced electromagnetic field. A current in the rotor is induced due to this field, which creates another field that tries to align with the stator field, causing the rotor to spin. A slip is created between these fields, when a load is applied to the motor. This rotor speed decreases at higher slip values. The no load speed is also called the synchronous speed. The frequency of the stator voltage controls the synchronous speed. The frequency of the voltage is applied to the stator through power electronic devices, which allows the control of the speed of the motor.

What is of interest is the motoring region of induction machines, when the slip is between 0 and 1, and the machine acts as a motor. This region is defined by the starting torque, τ_{start}, which is the torque required to overcome the inertia of the motor when it is at standstill and cause it to move; the maximum or pull-out torque, τ_{max}, which is the maximum torque that can be applied to the motor already in motion and cause it to stop; and the rated torque, τ_{rated}, which is the torque generated by the motor when it is operating at its rated speed, n_{rated}; the rated speed is usually has a slip of 0.9 or more. As can be observed, the torque begins to fall as slip increases, and attains a value of zero when the motor reaches the synchronous speed.

The research is using techniques, which implement a constant voltage to frequency ratio. The induction motor synchronous speed is defined by following equation:

$$n_s = \frac{120 f}{p} \quad (20)$$

where *f* is the frequency of AC supply, n_s is the synchronous speed of rotor; *p* is the number of poles per phase of the motor. By varying the frequency of control circuit through AC supply, the rotor speed will change. The mechanical or rotor speed, n_m, is defined by the slip, s:

$$s = \frac{n_s - n_m}{n_s}, \text{ or } n_m = (1 - s) * n_s \quad (21)$$

Finally, the torque equation is given by:

$$\tau = \frac{360\pi I_r^2 R_r}{s n_S} \tag{22}$$

where, Ir is the rotor current and Rr is the rotor resistance.

Table 5 Rating of Δ-connected 3-phase induction motor used for simulation.

Symbol	Definition of the Parameters	Value
R_s	Resistance of stator	2.94 Ω
L_s	Inductance of stator	10.5 mH
R_r	Resistance of rotor	1.75 Ω
L_r	Inductance of rotor	7.50 mH
L_m	Magnetizing inductance	41 mH
p	Pole number	6
J	Moment of inertia	0.41 kgm^2
P_M	Motor power	1 hp
V_{PH}	Phase voltage RMS	220 V
I_r	Current RMS	4.15 A
n_r	Rated speed	2,500 rpm

Figure 5 presents the schematic diagram of forward converter based proposed System with PSIM Software which runs the Induction Motor discussed in **Table 5**. Initially there is transient noise that is soon filtered out as motor approaches its rated speed.

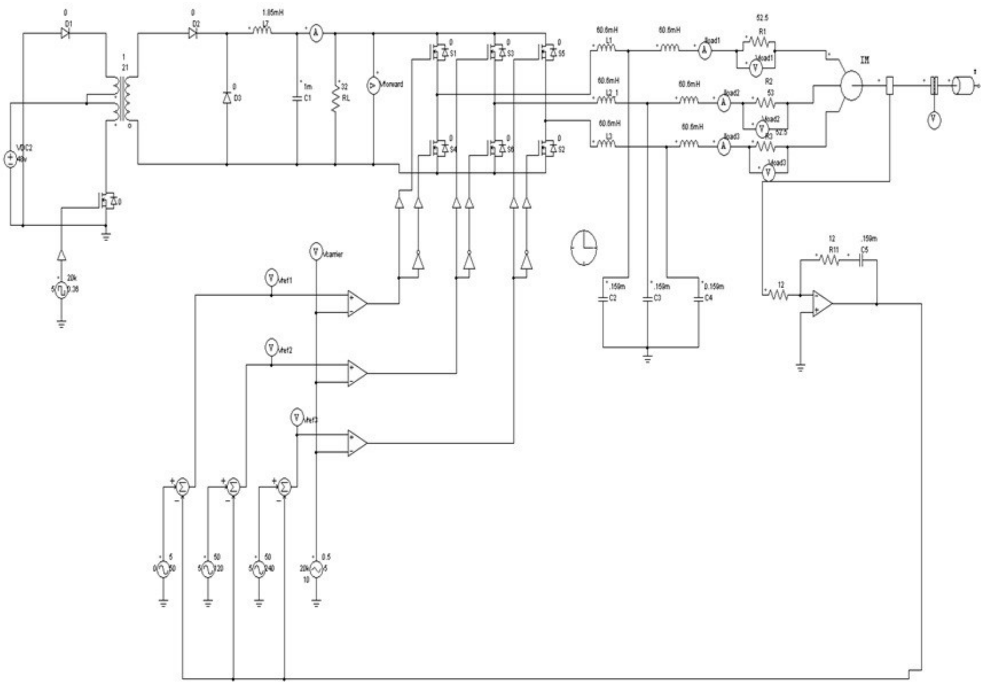

Figure 5 Forward converter based proposed system with induction motor in PSIM.

Economic analysis

The 4 hp Diesel engine used for irrigation purpose normally consumes 1,440 L diesel in a year [28]. The total installation cost is 2,91,000 BDT in the proposed system, annual maintenance cost is 2 % of the total capital investment. Induction Motor and Pump will be replaced after 10 years considering the life cycle. Similarly, the inverter system along with DC-DC Forward Converter will be replaced after 5 years. For life cycle cost analysis (LCCA), a timeframe of 20 years is considered. The other parameters are as follows, Inflation rate: 5.84 %, Annualization factor: 13.67, Discount rate: 10 %. [29].

Table 6 LCCA of Diesel engine-based system.

Components		**Unit**	**Size**	**Price in BDT**
(a) Diesel engine (including installation)		1	4 hp	40,960
(A) Capital cost (= a)				**40,960**
(B) Recurring Maintenance cost(= C + D)	Annual fuel (Diesel) cost, Ca1	Unit	Unit price (BDT)	93,600
		1,440 L (Per year)	65	
	Recurring factor, Pa1			13.67
	(C) Life cycle maintenance cost LCMC1(= Ca1*Pa1)			**12,79,512**
	Annual maintenance cost, Ca2 (10 % of capital cost)			4,096
	Recurring factor, Pa2			13.67
	(D) Life cycle maintenance cost LCMC2(= Ca2*Pa2)			**55,992.32**
(E) Non-recurring replacement cost	Diesel engine replacement, **Cr1** (after 10 Years) (= b)			40,960
	Non-recurring factor, Pr1 (10 Years)			0.68
	Life cycle replacement cost LCRC1(= Pr1*Cr1)			**27,852.8**
Total life cycle cost (= A + B + E)				**14,04,317.12**

Table 7 LCCA of forward converter and 3-phase SPWM inverter-based system.

Components		**Unit**	**Size**	**Price in BDT**
(a) PV panel cost			3.2 kW	1,92,000
(b) Induction motor and pump		1	3 hp	40,000
(c) Forward converter		1		4,000
(d) SPWM inverter and filter		1		18,000
(e) Installation (electrical and civil structure)				32,000
(f) Miscellaneous cost				5,000
(A) Total capital cost (= a + b + c + d + e + f)				**2,91,000**
(B) Recurring maintenance cost	Annual maintenance cost, Ca (2 % of capital cost)			5,820
	Recurring factor, Pa			13.67
	Life cycle maintenance cost LCMC(= Ca*Pa)			**79,559.4**
(C) Non-recurring replacement cost(= D + E)	Induction motor and pump replacement, **Cr1** (after 10 Years) (= b)			40,000
	Non-recurring factor, Pr1 (10 Years)			0.68
	(D) Life Cycle replacement cost LCRC1(= Pr1*Cr1)			**27,200**
	Forward converter, SPWM inverter and filter replacement, **Cr2** (after 5 Years) (= c + d)			22,000
	Non-recurring factor, Pr2 (5 Years)			0.82
	(E) Life cycle replacement cost LCRC2(= Pr2*Cr2)			**18,040**
Total life cycle cost (= A + B + C)				**4,15,799.4**

Result and discussion

Forward converter output voltage simulated in PSIM is 312V DC presented in **Figure 6**. The speed and torque characteristics of Δ-connected induction motor are illustrated in **Figure 7**.

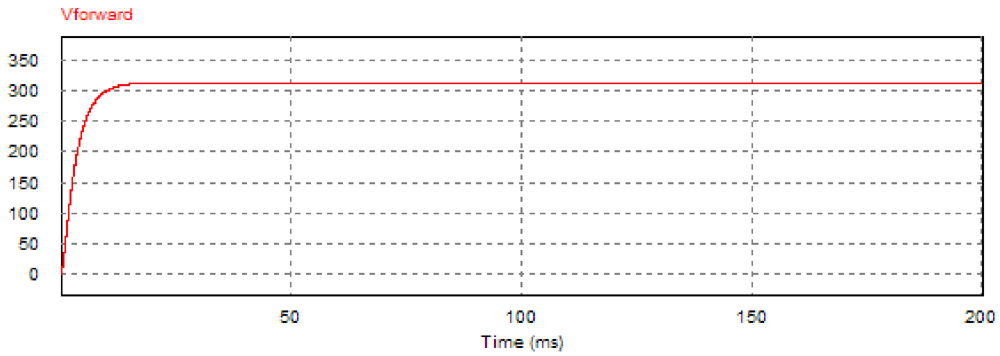

Figure 6 Forward converter output voltage.

Induction motor operation frequency is 150 Hz (3 times the grid frequency), and the slip at which the motor attains its rated speed of 2,500 rpm is 0.833. Thus, the rated torque can be calculated as 13.64 Nm. This fact is verified in speed characteristics and torque of induction motor simulated in PSIM illustrated in **Figure 7**.

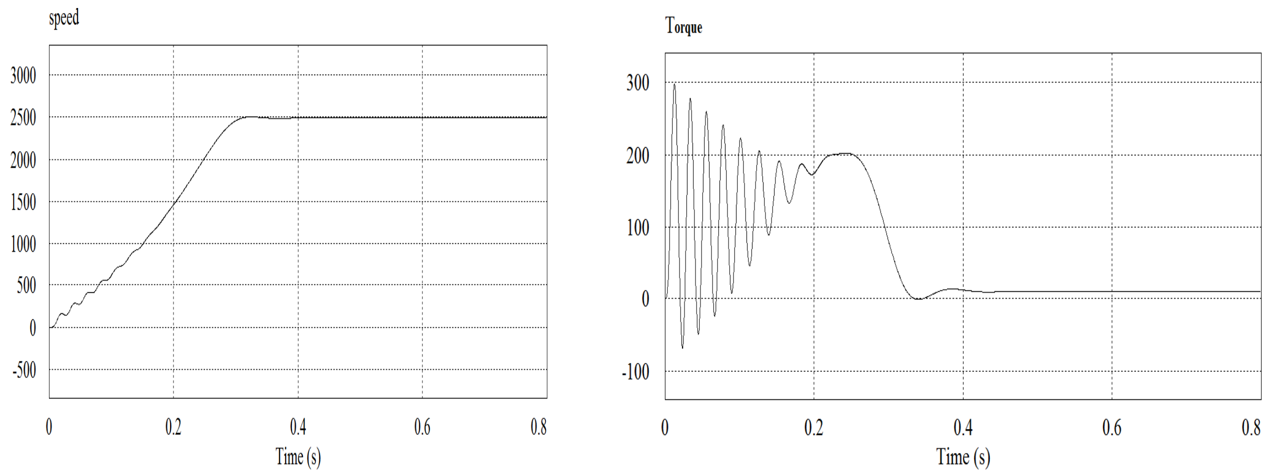

Figure 7 Speed characteristics and torque of induction motor in PSIM.

The bode plot of the T-LCL filter is presented in **Figure 8**. Result shows that the resonance frequency is around 4,750 KHz, where we have a magnitude of −34 dB, which corresponds to an attenuation of 2 % or 0.02.

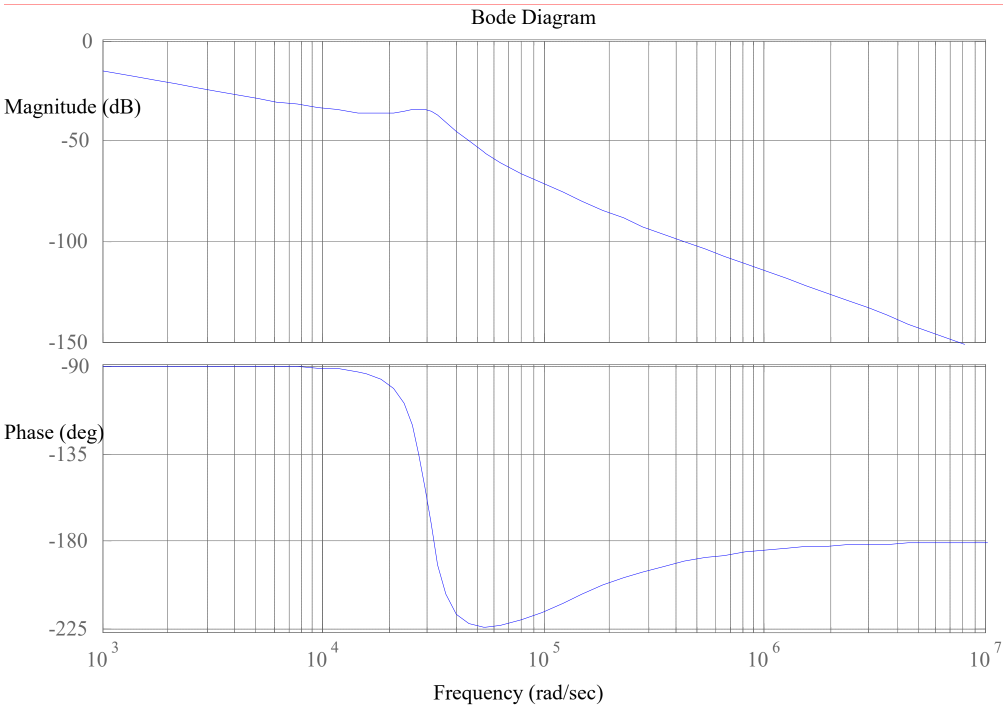

Figure 8 T-LCL filter Bode plot with 2 % damping resistance, 2 % attenuation and 10 % ripple current.

Figures 9(a) - 9(c) illustrates the waveform of simulated output voltage for the 3-phases Vr, Vg, Vb. These voltages are not sinusoidal; rather they are distorted. Harmonics reduction is ensured by introducing the filter at inverter output as mentioned earlier. **Figure 10(a)** presents the 3-phase sinusoidal output voltage and **Figure 10(b)** illustrates the waveform of Inverter output current.

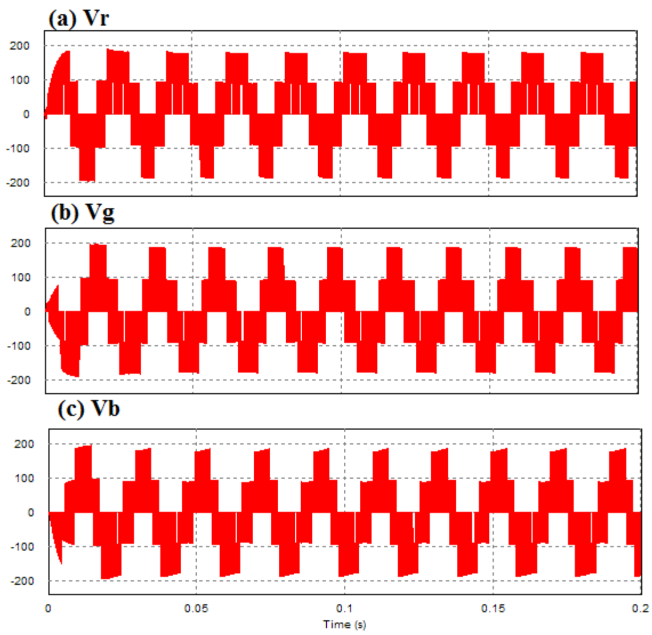

Figure 9 3-phase PWM output voltage (without filter).

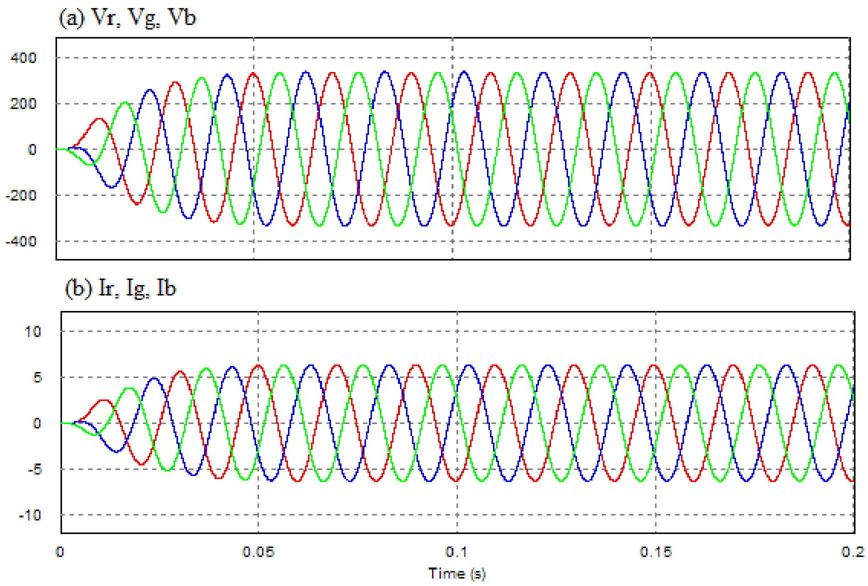

Figure 10 (a) 3-phase output voltage and (b) output current (with filter).

The basic comparison between simulation result of forward converter based proposed system and conventional System such as step-up transformer can be describe from the following 2 tables. For the same cell voltage, parameters like output rms voltage, output rms current and output rms power is calculated. Though T-LCL filter is introduced in both the cases, but the THD is improved to 0.087 in forward converter-based system, where the THD level is 0.103 in conventional transformer-based system.

Table 8 Simulation result of 3-phase SPWM inverter with forward converter.

Cell voltage	Output voltage (rms value)	Output current (rms value)	Output power (rms value)	THD (with T-LCL filter)
12	55.10	1.03	57.29	0.087
24	110.15	2.07	228.74	0.087
48	220.09	4.15	914.02	0.087
60	275.10	5.19	1428.05	0.087
96	440.17	8.30	3655.89	0.087

Table 9 Simulation result of 3-phase SPWM inverter with transformer.

Cell voltage	Output voltage (rms value)	Output current (rms value)	Output power (rms value)	THD (with T-LCL Filter)	Efficiency (%)
12	54.99	1.24	68.61	0.103	82.64872
24	109.98	2.49	274.43	0.103	82.64647
48	219.96	4.98	1097.58	0.103	82.64164
60	275.46	6.23	1717.52	0.103	82.63038
96	440.98	9.97	4399.32	0.773	82.69347

Conclusions

As geographical position of Bangladesh which is lying in north-eastern part of South Asia receiving sunlight in a good amount of period in a day, the average bright sunshine period is 7.6 h, implementation water pumping system which is fed by solar energy can be a good solution considering the decreased price of solar panel. Though the capital investment of the solar system is quite high but the price of solar panels is gradually decreasing in the international market. This indicates that the solar based irrigation system will be more feasible in the upcoming years. The analysis is made for 20 years. From **Table 8**, it is calculated that the total life cycle cost for conventional Diesel based water pump is 14,04,317.12 BDT, where Life Cycle cost for proposed photovoltaic irrigation pumping system is 4,15,799.4 BDT in **Table 9**. Over the time, due to continuous research and development in the field of photovoltaic panel and advancement in manufacturing will reduce the component costs and make the system more economical in the future.

References

[1] EI Ortiz-Rivera. Maximum power point tracking using the optimal duty ratio for DC-DC converters and load matching in photovoltaic application. *In*: Proceedings of the 23rd Annual IEEE Applied Power Electronics Conference and Exposition, Texas, United States. 2008, p. 987-91.

[2] HK Shakir-Ul, T Rahman and MS Hossain. A brief study of the prospect of solar energy in generation of electricity in Bangladesh. *Cyber J.* 2012; **6**, 1-8.

[3] DH Muhsenab, T Khatib and F Nagi. A review of photovoltaic water pumping system designing methods, control strategies and field performance. *Renew. Sustain. Energ. Rev*. 2017; **68**, 70-86.

[4] CLP Swamy, B Singh, BP Singh and SS Murthy. Experimental investigations on a permanent magnet brushless DC motor fed by PV array for water pumping system. *In*: Proceedings of the 31st Intersociety Energy Conversion Engineering Conference, Washington, United States. 1996, p. 1663-8.

[5] A Elamathy and G Vijayagowril. Multiport DC-DC interleaved boost converter supplemented by hybrid system of different capacities PV and battery power system. *In*: Proceedings of the 2nd International Conference on Electronics and Communication Systems, Coimbatore, India. 2015, p. 921-5.

[6] MR Feyzi, SAKM Niapour, F Nejabatkhah, S Danyali and A Feizi. Brushless DC motor drive based on multi-input DC boost converter supplemented by hybrid PV/FC/battery power system. *In*: Proceedings of the 24th Canadian Conference on Electrical and Computer Engineering, Ontario, Canada. 2011, 000442-6.

[7] N Mendez-Gomez, O Bousono, R Castaneyra and EI Ortiz-Rivera. Development of a low-cost induction motor drive system using a PVM, boost converter and three-phase inverter. *In*: Proceedings of the 38th IEEE Photovoltaic Specialists Conference, Texas, United States. 2012, p, 1348-51.

[8] S Biswas and MT Iqbal. Dynamic modelling of a solar water pumping system with energy storage. *J. Sol. Energ.* 2018; **2018**, 8471715.

[9] R Kumar and B Singh. BLDC motor driven water pump fed by solar photovoltaic array using boost converter. *In*: Proceedings of the 2015 Annual IEEE India Conference, New Delhi, India. 2015, p. 1-6.

[10] RK Rao, P Srinivas and S Kranthikumar. Simulation and analysis of electrical water pumping system using solar energy. *In*: Proceedings of the 2014 International Conference on Smart Electric Grid, Guntur, India. 2014, p. 1-6.

[11] MA Razzak, ASK Chowdhury and KMA Salam. Induction motor drive system using push-pull converter and three-phase SPWM inverter fed from solar photovoltaic panel. *In*: Proceedings of the 2014 Power and Energy Systems: Towards Sustainable Energy, Bangalore, India. 2014, p. 1-6.

[12] DLD Moral, A Barrado, M Sanz, A Lázaro, C Fernandez and P Zumel. High efficiency DC-DC autotransformer forward-flyback converter for DMPPT architectures in solar plants. *In*: Proceedings of the 9th International Conference on Compatibility and Power Electronics, Costa da Caparica, Portugal. 2015, p. 431-6.

[13] E Ortiz-Perez, R Maldonado, H O'Neill and EI Ortiz-Rivera. Proposed system model and simulation for three-phase induction motor operation with single PV panel. *In*: Proceedings of the 2011 IEEE Power and Energy Society General Meeting, Michigan. 2011, p. 1-6.

[14] UK Kalla, N Bhati, K Chariya and I Qureshi. Design and analysis of solar PV fed IMD water - pumping system. *In*: Proceedings of the 2021 International Conference on Sustainable Energy and Future Electric Transportation, Hyderabad, India. 2021, p. 1-6.
[15] D Holmes, P Atmur, C Beckett, M Bull, W Luo, D Ng, N Sachchithananthan, P Su, D Ware and P Wrzos. An innovative efficient current-fed push-pull grid connectable inverter for distributed generation systems. *In*: Proceedings of the 37th IEEE Power Electronics Specialists Conference, Jeju, Korea. 2006, p. 1-7.
[16] JA Santiago-Gonzalez, J Cruz-Colon, R otero-De-leon, V lopez- Santiago and EI Ortiz-Rivera. Three phase induction motor drive using flyback converter and PWM inverter fed from a single photovoltaic panel. *In*: Proceedings of the 2011 IEEE Power and Energy Society General Meeting, Michigan, United States. 2011, p. 1-6.
[17] J Košičan, MÁP Picazo, S Vilčeková and D Košičanová. Life cycle assessment and economic energy efficiency of a solar thermal installation in a family house. *Sustainability* 2021; **13**, 2305.
[18] EG Shivakumar, K Gopakumar, SK Sinha, A Pittet and VT Ranganathan. Space vector PWM control of dual inverter fed open-end winding induction motor drive. *In*: Proceedings of the 16th Annual IEEE Applied Power Electronics Conference and Exposition, California, United States. 2001, p. 399-405.
[19] JM Erdman, RJ Kerkman, DW Schlegel and GL Skibinski. Effect of PWM inverters on AC motor bearing currents and shaft voltages. *IEEE Trans. Ind. Appl*. 1996; **32**, 250-9.
[20] S Srinivas and VT Somasekhar. A new-alternate inverter PWM switching strategy for reducing the common-mode voltages for a dual-inverter fed open-end winding induction motor drive. *In*: Proceedings of the 2005 International Power Electronics Conference, Niigata, Japan. 2005, p. 1460-3.
[21] PJ Sudarshan, KMC Swamy, P Nagaraja and J Manohar. A novel transformer less SPWM inverter using DC-DC boost converter with coupled inductor for standalone applications. *In*: Proceedings of the 2016 International Conference on Computation of Power, Energy Information and Commuincation, Melmaruvathur, India. 2016, p. 581-6.
[22] M Rashid. *Power electronics: Circuits, devices, and applications*. Pearson, London, 2013, p. 1-1024.
[23] MS Hossain, SMB Billah, S Barua, MS Mahmud and T Khadem. Life cycle cost analysis of solar-LED alternatives to fuel-based fishing net indicator. *In*: Proceedings of the 2017 International Conference on Innovations in Green Energy and Healthcare Technologies, Coimbatore, India. 2017, p. 1-4.
[24] M Milousi, M Souliotis, G Arampatzis and S Papaefthimiou. Evaluating the environmental performance of solar energy systems through a combined life cycle assessment and cost analysis. *Sustainability* 2019; **11**, 2539.
[25] N Mohan, TM Undeland and WP Robbins. *Power Electronics*. *In*: SM Elliot, SM Culhane, S Elbe, S Amanatidis, L Rogan, D Levy, L Bulwin and J Perea (Eds.). John Wiley & Sons, New York, 1995, p. 1-802.
[26] PS Bimbhra. *Power electronics*. Khanna Publisher, New Delhi, India, 2012, p. 1-916.
[27] MD Singh and KB Khanchandani. *Power electronics*. Tata McGraw Hill, New Delhi, India, 2007, p. 1-1071.
[28] S Chakraborty, W Hasan and SMB Baque. Design and analysis of a transformer-less single-phase grid-tie photovoltaic inverter using boost converter with Immittance conversion topology. *In*: Proceedings of the 2014 International Conference on Electrical Engineering and Information & Communication Technology, Dhaka, Bangladesh. 2014, p. 1-6.
[29] Z Tasneem, SI Annie and KM Salim. Economic analysis of a 3KW solar based irrigation system and comparison with its Diesel based counterpart. *In*: Proceedings of the 2015 IEEE International WIE Conference on Electrical and Computer Engineering, Dhaka, Bangladesh. 2015, p. 14-7.
[30] X Renzhong, X Lie, Z Junjun and D Jie. Design and research on the LCL filter in three-phase PV grid-connected inverters. *Int. J. Comput. Electr. Eng.* 2013; **5**, 322-5.
[31] Y Tang, W Yao, PC Loh and F Blaabjerg. Design of LCL filters with LCL resonance frequencies beyond the nyquist frequency for grid-connected converters. *In*: Proceedings of the 2015 IEEE Energy Conversion Congress and Exposition, Quebec, Canada. 2015, p. 5137-44.
[32] UP Yagnik and MD Solanki. Comparison of L, LC & LCL filter for grid connected converter. *In*: Proceedings of the 2017 International Conference on Trends in Electronics and Informatics, Tirunelveli, India. 2017, p. 455-8.